



# Topological Shape Optimization Scheme for Nonlinear Structures Based on Artificial Bee Colony Algorithm

Yong-Ho Kim<sup>a</sup>, Seog-Young Han<sup>a\*</sup><sup>a</sup> School of Mechanical Engineering, Hanyang University, 222 Wangsimni-ro, Seongdong-gu, Seoul 04763, Korea

## ARTICLE INFO

### Article history:

Received	3	April	2018
Revised	1	June	2018
Accepted	3	August	2018

### Keywords:

Artificial bee colony algorithm  
Topological shape optimization  
Nonlinear structures  
Boundary elements

## ABSTRACT

This paper suggests a topological shape optimization scheme for nonlinear structures considering geometrically, materially and both geometrically and materially nonlinear cases based on an artificial bee colony algorithm (ABCA). To perform a topological shape optimization of nonlinear problems, a variable called "Improved Boundary Element Indicator (IBEI)" is introduced to define the boundary elements in each iteration. Typical examples consider three kinds of nonlinear cases, and it can be verified that the IBEI is suitable for topological shape optimization for linear and nonlinear structures. It can then be found that the suggested method can naturally create holes in the structure without any initial holes or topological sensitivity, although only the boundary elements are optimized. Finally, we conclude that convergence rate of the suggested ABCA is improved to more than 60% of the discrete level set method (LSM) and 5% of the ABCA for topology optimization (except for the geometrically nonlinear case).

## 1. Introduction

Topological shape optimization is particularly efficient because it can perform topology and shape optimizations simultaneously. Topology optimization operates by finding an optimized layout in the specified design domain under the required conditions, such as boundary and loading conditions. Shape optimization is then used to obtain an optimal shape using design variables indicating the shape of the structure. Sethian and Wiegmann<sup>[1]</sup> first developed a topological shape optimization method. They proposed the level set method (LSM) for the boundary design of elastic structures with topological changes. Bourdin and Chambolle<sup>[2]</sup> developed the phase field method (PFM) for topological shape optimization. The optimized structure based on the PFM is represented as

a subset of a reference domain, and the complement of the subset is made of two other phases, the void and a fictitious liquid that exerts a pressure force on its interface with a solid structure. Due to the substantial performance of the LSM and the PFM, the methods are employed for various engineering problems for topological shape optimization<sup>[1-7]</sup>.

When solving linear static stiffness problems, it is usually assumed that the material of a structure is linear and deformation is small<sup>[8]</sup>. However, when an applied load or deformation of the structure is very large, geometric nonlinearity may occur. Also, when a structure is made with nonlinear material, material nonlinearity may occur, and sometimes these two kinds of nonlinearities can occur simultaneously<sup>[8]</sup>. Therefore, the above nonlinearities should be considered in order to optimize the nonlinear structures

\* Corresponding author. Tel.: +82-2-2220-0456

Fax: +82-2-2220-2299

E-mail address: syhan@hanyang.ac.kr (Seog-Young Han).

appropriately.

Kwak and Cho<sup>[9]</sup> developed the topological shape optimization method for geometrically nonlinear structures in total Lagrangian formulation using the LSM. This method minimizes the compliance through the variations of implicit boundary, satisfying an allowable volume of Lagrangian derived from an optimality condition. Total Lagrangian formulation was employed to obtain the response of geometrically nonlinear structures, and the Newton-Raphson iterative scheme was used to solve the nonlinear systems. Cho et al.<sup>[10]</sup> employed the topological derivatives to perform the topological shape optimization of geometrically nonlinear structures based on the LSM. This method can create new holes whenever and wherever necessary during the optimization and minimize the compliance using both shape and topological variations simultaneously. Also, Ha and Cho<sup>[11]</sup> proposed an unstructured mesh for the topological shape optimization method of geometrically nonlinear structures using the LSM. The method can be relieved by the convergence difficulty because homogeneous material property and actual boundary are employed.

Penzler et al.<sup>[12]</sup> developed the PFM for topological shape optimization in nonlinear elasticity. In the research, the geometrically nonlinear deformations and nonlinear hyperelastic constitutive laws were considered. The resulting nonlinear elastic optimization problem differs significantly from classical optimization in linearized elasticity. Myśliński and Koniarski<sup>[13]</sup> combined the LSM and the PFM to consider the topological shape optimization problem for the elastic contact problem with prescribed friction condition numerically. The obtained numerical results indicated that the method allows for significant improvements in the solution from one iteration to the next, and is more efficient than the classical LSM.

To maximize the structural stiffness considering the nonlinearities, the displacement or compliance is naturally selected as an objective function. However, in the nonlinear static stiffness problems, minimization of the compliance may result in degenerated structures that can only support the maximum load for which they are designed. To avoid this problem and make sure that the structure is stable for any load up to the maximum design load, the complementary work as the objective function was suggested<sup>[8]</sup>.

Recently, Karaboga and Basturk<sup>[14]</sup> verified that the artificial bee colony algorithm (ABCA), which is based on swarms of

honey bees searching for food sources, converges to a global optimum more rapidly than other optimization algorithms such as the differential evolution (DE) algorithm<sup>[15]</sup>, particle swarm optimization (PSO) algorithm<sup>[16]</sup> and evolutionary algorithm (EA)<sup>[17]</sup>. Due to its outstanding performance, the ABCA has been employed for various engineering problems such as the inverse kinematics problem of robot arms<sup>[18]</sup>, layer optimization of symmetrical laminated composite plates<sup>[19]</sup>, structural shape optimization for static stiffness problems<sup>[20,21]</sup> and structural topology optimization for linear and nonlinear static and dynamic stiffness problems<sup>[22-24]</sup>.

The existing methods for topological shape optimization such as the LSM and the PFM have some problems. They cannot create new holes naturally without the initial holes or topological sensitivity<sup>[3,6,25]</sup>. Also, the convergence rates of the existing methods are slow because the geometry can only be evolved from an existing boundary region. Therefore, a new method for topological shape optimization based on the ABCA is suggested.

In this study, a topological shape optimization scheme for the nonlinear structures considering geometrically, materially and both geometrically and materially nonlinear cases using the ABCA is suggested. Since the suggested ABCA can create new holes in the structure naturally, unlike the LSM and the PFM, it is expected that the ABCA will be efficient for solving nonlinear problems as well as linear problems. To perform the topological shape optimization of nonlinear problems, a variable called "Improved Boundary Element Indicator (IBEI)" is newly introduced to define the boundary elements in each iteration. Finally, in order to examine the performance of the proposed method, numerical examples of typical nonlinear problems are provided. These examples compare the discrete LSM<sup>[25]</sup>, which is the existing method for topological shape optimization, ABCA for topology optimization<sup>[22-24]</sup>, and ABCA for topological shape optimization, which is the suggested method in this paper.

## 2. Formulation for Nonlinear Topological Shape Optimization

### 2.1 Problem Statement

In this paper, the complementary work is chosen as the objective function for topological shape optimization of nonlinear structures. The problem's statement is as follows:

$$\text{Minimize : } W^C = \lim_{l \rightarrow \infty} \frac{1}{2} \sum_{i=1}^l (\mathbf{f}_i^T - \mathbf{f}_{i-1}^T)(\mathbf{u}_i + \mathbf{u}_{i-1})$$

Subject to : Equilibrium equation

$$V^* - \sum_{e=1}^N V_e \chi_e = 0$$

$$\chi_e = \begin{cases} 1 & (\text{for solid element}) \\ \chi_{\min} & (\text{for void element}) \end{cases} \quad (1)$$

where  $W^C$  is the complementary work,  $l$  is the total number of load increments,  $T$  is the transpose,  $\mathbf{f}_i$  is the applied load vector of the  $i$ -th load increment,  $\mathbf{u}_i$  is the nodal displacement vector of the  $i$ -th load increment,  $V^*$  is the prescribed volume constraint,  $N$  is the total number of elements in the design domain,  $V_e$  is the volume of the  $e$ -th element,  $\chi_e$  is the binary design variable of  $e$ -th element, and  $\chi_{\min}$  is the sufficiently small value of the  $\chi_e$  to avoid singularity.

## 2.2 Sensitivity Number Using Waggle Index Update Rule

Kaveh et al.<sup>[26]</sup> employed the pheromone that is the intermediate variable for topology optimization using the ant colony optimization (ACO) algorithm. In the ABCA for topology optimization<sup>[22-24]</sup>, the waggle index update rule, which is inspired by the research of Kaveh et al.<sup>[26]</sup>, was also applied to the calculation of the sensitivity number. In this study, the waggle index update rule is also employed to obtain the sensitivity number. The waggle index update rule is expressed as:

$$I_e^k = \delta \times I_e^{k-1} + (1 - \delta) \times e_e^k \quad (2)$$

where  $I_e$  is the waggle index (the amount of information shared on the  $e$ -th element),  $e_e$  is the employed bee presence/absence,  $k$  is the current iteration number, and  $\delta$  is the coefficient of the waggle index update.

To obtain the sensitivity number, an adjoint equation is developed by using a series of vectors of Lagrangian multipliers  $\lambda_i$  into the  $W^C$  in Eq. (1) as<sup>[8]</sup>:

$$W^C = \lim_{l \rightarrow \infty} \frac{1}{2} \sum_{i=1}^l [(\mathbf{f}_i^T - \mathbf{f}_{i-1}^T)(\mathbf{u}_i + \mathbf{u}_{i-1}) + \lambda_i^T (\mathbf{r}_i + \mathbf{r}_{i-1})] \quad (3)$$

where  $\mathbf{r}_i$  is the residual force of  $i$ -th load increment.

$\mathbf{r}_i + \mathbf{r}_{i-1}$  is as follows:

$$\mathbf{r}_i + \mathbf{r}_{i-1} = \mathbf{f}_i - \mathbf{f}_i^{\text{int}} + \mathbf{f}_{i-1} - \mathbf{f}_{i-1}^{\text{int}} = 0 \quad (4)$$

where  $\mathbf{f}_i^{\text{int}}$  is the internal load of the  $i$ -th load increment. The sensitivity of Eq. (3) can be obtained as follows:

$$\frac{\partial W^C}{\partial \chi_e} = \lim_{l \rightarrow \infty} \frac{1}{2} \sum_{i=1}^l \left[ (\mathbf{f}_i^T - \mathbf{f}_{i-1}^T) \left( \frac{\partial \mathbf{u}_i}{\partial \chi_e} + \frac{\partial \mathbf{u}_{i-1}}{\partial \chi_e} \right) + \lambda_i^T \left( \frac{\partial \mathbf{r}_i}{\partial \mathbf{u}_i} \frac{\partial \mathbf{u}_i}{\partial \chi_e} + \frac{\partial \mathbf{r}_{i-1}}{\partial \mathbf{u}_{i-1}} \frac{\partial \mathbf{u}_{i-1}}{\partial \chi_e} + \frac{\partial (\mathbf{r}_i + \mathbf{r}_{i-1})}{\partial \chi_e} \right) \right] \quad (5)$$

If the increment of the load is small enough, the relationship between the load and displacement can be assumed to be linear, where  $\partial \mathbf{r}_i / \partial \mathbf{u}_i$  and  $\partial \mathbf{r}_{i-1} / \partial \mathbf{u}_{i-1}$  can be expressed using the tangential stiffness matrix  $\mathbf{K}_i^t$  at the  $i$ -th load increment as follows:

$$\frac{\partial \mathbf{r}_i}{\partial \mathbf{u}_i} = \frac{\partial \mathbf{r}_{i-1}}{\partial \mathbf{u}_{i-1}} = -\mathbf{K}_i^t \quad (6)$$

The sensitivity of the complementary work can be rewritten as Eq. (7) by applying Eq. (6) to Eq. (5).

$$\frac{\partial W^C}{\partial \chi_e} = \lim_{l \rightarrow \infty} \frac{1}{2} \sum_{i=1}^l \left[ (\mathbf{f}_i^T - \mathbf{f}_{i-1}^T - \lambda_i^T \mathbf{K}_i^t) \left( \frac{\partial \mathbf{u}_i}{\partial \chi_e} + \frac{\partial \mathbf{u}_{i-1}}{\partial \chi_e} \right) + \lambda_i^T \frac{\partial (\mathbf{r}_i + \mathbf{r}_{i-1})}{\partial \chi_e} \right] \quad (7)$$

In order to remove the  $(\partial \mathbf{u}_i / \partial \chi_e + \partial \mathbf{u}_{i-1} / \partial \chi_e)$  term, the Lagrangian multiplier is calculated as follows:

$$\lambda_i \mathbf{K}_i^t = \mathbf{f}_i^T - \mathbf{f}_{i-1}^T = \mathbf{K}_i^t (\mathbf{u}_i - \mathbf{u}_{i-1}) \quad (8)$$

$$\lambda_i = \mathbf{u}_i - \mathbf{u}_{i-1} \quad (9)$$

Based on Eqs. (8) and (9), the sensitivity of the complementary work can be expressed as:

$$\frac{\partial W^C}{\partial \chi_e} = \lim_{l \rightarrow \infty} \frac{1}{2} \sum_{i=1}^l \left[ \lambda_i^T \frac{\partial (\mathbf{r}_i + \mathbf{r}_{i-1})}{\partial \chi_e} \right] = -\lim_{l \rightarrow \infty} \frac{1}{2} \sum_{i=1}^l \left[ (\mathbf{u}_i^T - \mathbf{u}_{i-1}^T) \left( \frac{\partial \mathbf{f}_i^{\text{int}}}{\partial \chi_e} + \frac{\partial \mathbf{f}_{i-1}^{\text{int}}}{\partial \chi_e} \right) \right] \quad (10)$$

In the case of material nonlinearity, a general relationship between the effective stress and the effective strain can be represented as follows:

$$\sigma^{\text{eff}} = K_c \Phi(\varepsilon^{\text{eff}}) \quad (11)$$

where  $\sigma^{\text{eff}}$  is the effective stress,  $K_c$  is the constant related to

the elastic modulus,  $\Phi(\varepsilon^{\text{eff}})$  is the general function representing the material characteristics, and  $\varepsilon^{\text{eff}}$  is the effective strain.

In the power-law model,  $\Phi(\varepsilon^{\text{eff}})$  is expressed using the work-hardening exponent  $m$ , and the material interpolation scheme is introduced in order to consider solid and void elements. The effective stress  $\sigma^{\text{eff}}(\chi_e)$  of each element can be written as follows:

$$\sigma^{\text{eff}}(\chi_e) = \chi_e^p K_c \Phi(\varepsilon^{\text{eff},1}) \quad (12)$$

where  $p$  is the penalty factor,  $\varepsilon^{\text{eff},1}$  is the effective strain of solid element.

Internal load for  $e$ -th element becomes as follows:

$$\mathbf{f}_e^{\text{int}} = \sum_{e=1}^N \chi_e^p \mathbf{C}^{eT} \mathbf{f}^{\text{int},1} \quad (13)$$

where  $\mathbf{f}_e^{\text{int}}$  is the internal load vector for  $e$ -th element,  $\mathbf{C}^e$  is the matrix which transforms the nodal force vector of an element to the global nodal force vector,  $\mathbf{f}^{\text{int},1}$  is the internal load vector of solid element.

Substituting Eq. (13) into Eq. (10), the following equation can be obtained as:

$$\frac{\partial W^C}{\partial \chi_e} = -\lim_{l \rightarrow \infty} \frac{1}{2} p \chi_e^{p-1} \sum_{i=1}^l (\mathbf{u}_i^T - \mathbf{u}_{i-1}^T) (\mathbf{C}^{eT} \mathbf{f}_{e,i}^{\text{int}} + \mathbf{C}^{eT} \mathbf{f}_{e,i-1}^{\text{int}}) \quad (14)$$

where  $\mathbf{f}_{e,i}^{\text{int}}$  is the internal load vector of solid element in the  $i$ -th load increment.

The (-) sign indicates that the complementary work is reduced as the design variable  $\chi_e$  is increased. In order to minimize the complementary work, the sensitivity number of the  $e$ -th element can be represented as follows:

$$\begin{aligned} \alpha_e &= -\frac{1}{p} \frac{\partial W^C}{\partial \chi_e} \\ &= \chi_e^{p-1} \lim_{l \rightarrow \infty} \frac{1}{2} \sum_{i=1}^l (\mathbf{u}_i^T - \mathbf{u}_{i-1}^T) (\mathbf{C}^{eT} \mathbf{f}_{e,i}^{\text{int}} + \mathbf{C}^{eT} \mathbf{f}_{e,i-1}^{\text{int}}) \\ &= \chi_e^{p-1} \lim_{l \rightarrow \infty} \sum_{i=1}^l (E_{e,i} - E_{e,i-1}) \\ &= \chi_e^{p-1} E_e \quad \chi_e = \begin{cases} 1 & (\text{for solid element}) \\ \chi_{\min} & (\text{for void element}) \end{cases} \quad (15) \end{aligned}$$

where  $E_e$  is the final elastic and plastic strain energy of the  $e$ -th element.

To perform the ABCA for topological shape optimization, the waggle index, which is the intermediate variable, should

be used for calculation of the sensitivity number. Therefore, the sensitivity number based on the waggle index update rule is as follows:

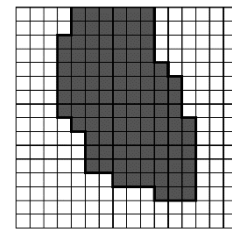
$$\alpha_e = I_e^{p-1} E_e \quad (0 < I_{\min} \leq I_e \leq 1) \quad (16)$$

where  $I_{\min}$  is a sufficiently small value of the  $I_e$  to avoid singularity.

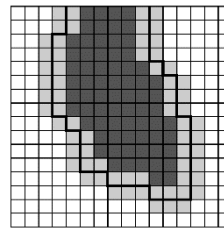
### 2.3 Improved Boundary Element Indicator

In order to perform topology and shape optimizations simultaneously (topological shape optimization), the boundary - including the creation of new holes in the structure - should be optimized. To define the boundary elements of the structure, the boundary element indicator (BEI) is employed. Once a structure is given as shown in Fig. 1(a), the boundary elements that are locations of the searching domain are defined using BEI as shown in Fig. 1(b). In this figure, the thick line is the boundary line, which is defined by the interface of solid and void elements. The black and white elements are solid and void elements respectively, and the grey elements are boundary elements. Both solid and void elements that are on each layer at both sides of the boundary line are defined as the boundary elements.

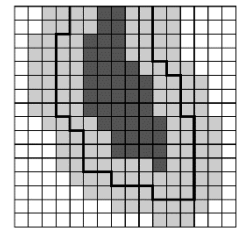
If the locations of boundary elements are defined continuously using the BEI in each iteration, holes can be created naturally and an approximate topology can be made. After an approximate topology is made, shape optimization is only



(a) Given structure







(b) Definition of the boundary elements based on the BEI



(c) Definition of the boundary elements based on the IBEI

**Fig. 1 Definition of the boundary elements based on the BEI and the IBEI**

**Table 1 Comparison of optimized designs using the suggested method based on both BEI and IBEI**

Linear / Nonlinear case	Suggested method based on the BEI	Suggested method based on the IBEI
Linear	 Iter. : 39 Obj. : 1.7144 J	 Iter. : 40 Obj. : 1.7107 J
Geometrically nonlinear	 Iter. : 45 Obj. : 1.6081 J	 Iter. : 48 Obj. : 1.5873 J

carried out because further new holes in the structure cannot be created. Through the above procedure, the topological shape optimization can be carried out, although only the shape optimization is performed.

When solving the linear problems using the BEI, the solutions are well searched, but it was verified through numerical experiments that nonlinear problems cannot be solved because the narrow searching domain is not sufficient to find a solution. In order to expand the searching domain, this paper suggests IBEI.

The difference between the BEI and IBEI is just the number of defined layers. Specifically, while the boundary elements based on the BEI are defined on each layer at both sides of the boundary line, those based on the IBEI are defined on the double layers at both sides of the boundary line. Fig. 1(c) shows the defined boundary elements based on the IBEI instead of the BEI. The IBEI is expressed as the following equation:

$$IBEI_e = \begin{cases} +1 & \text{(if it is a boundary element)} \\ -1 & \text{(if it is not a boundary element)} \end{cases} \quad (17)$$

where  $IBEI_e$  is the improved boundary element indicator of the  $e$ -th element.

Table 1 represents the optimized designs of the ABCA for topological shape optimization based on both BEI and IBEI. From the table, it can be found that both linear and geometrically nonlinear problems can be well solved using the IBEI. Hence, it can be concluded that the IBEI is applicable to various problems, such as linear and nonlinear problems.

### 3. ABCA for Nonlinear Topological Shape Optimization

The ABCA is applied to the topological shape optimization of nonlinear structures in this study. The procedure for topological shape optimization of nonlinear structures is suggested as:

Step 1: Establish the design domain based on rectangular finite elements and initial parameters for topological shape optimization.

Step 2: Perform finite element analysis (FEA) for the initial design and calculate the sensitivity number  $\alpha_e$  using Eq. (16).

Step 3: Calculate the temporary fitness value  $temp\_fit_e$  using the following equation.

$$temp\_fit_e = \begin{cases} \frac{1}{1+\alpha_e} & \text{(if } \alpha_e \geq 0) \\ 1+abs(\alpha_e) & \text{(if } \alpha_e < 0) \end{cases} \quad (18)$$

where  $abs(x)$  is the absolute value of  $x$ .

Step 4: Perform the employed bee phase for the topological shape optimization. In this step, the boundary elements should be updated continuously whenever a temporary candidate solution is found using Eq. (19). By using the equation, the  $temp\_fit_e$  is divided into two groups. If the fitness value  $fit_e$  is a positive value, the  $e$ -th element is a boundary element. Otherwise, the  $e$ -th element is not a boundary element. After that, determine the  $x_i, x_k$  (locations of initial solutions) and  $v_i$  (location of a temporary candidate solution) based on Eq. (20). In the equation,  $x_i, x_k$  and  $v_i$  should be a positive value for topological shape optimization.

$$fit_e = IBEI_e \times temp\_fit_e \quad (19)$$

$$\begin{aligned} v_i &= x_i + int[ rand[0,1] \times abs[x_i - x_k] ] \\ x_i &= int[ rand[0,1] \times sum[ IBEI_e > 0 ] ] \\ x_k &= int[ rand[0,1] \times sum[ IBEI_e > 0 ] ] \end{aligned} \quad (20)$$

$x_i, x_k, \text{ and } v_i \text{ for } fit_e > 0$

where  $fit_e$  is the fitness value of  $e$ -th element,  $int[x]$  is the integer number of  $x$ ,  $rand[a,b]$  is the random number between  $a$  and  $b$ ,  $sum[x]$  is the summation of  $x$ .

Step 5: Perform the onlooker bee phase for topological shape optimization. In this step, the  $IBEI_e$  and  $fit_e$  should be also updated using Eqs. (17) and (19), as in Step 4. Also, the

$x_i'$ ,  $x_k'$  (locations of newly selected initial solutions) and  $v_i'$  (location of a newly selected temporary candidate solution) are searched based on Eq. (21).

$$\begin{aligned}
 v_i' &= x_i' + \text{int} \left[ \text{rand} [0,1] \times \text{abs} [x_i' - x_k'] \right] \\
 &\quad \text{for } \text{rand} [0,1] < p_e \\
 x_i' &= \text{int} \left[ \text{rand} [0,1] \times \text{sum} [IBEI_e > 0] \right] \\
 x_k' &= \text{int} \left[ \text{rand} [0,1] \times \text{sum} [IBEI_e > 0] \right] \\
 x_i', x_k', \text{ and } v_i' &\text{ for } \text{fit}_e > 0 \\
 p_e &= \frac{\text{fit}_e}{\sum_{e=1}^N \text{fit}_e} \quad (21)
 \end{aligned}$$

where  $p_e$  is the probability value of  $e$ -th element.

Step 6: Perform the scout bee phase. Specify the elements occupied and abandoned by employed bees (solid and void elements) using the fitness value of each element. After that, the locations of solid and void elements should be determined based on the prescribed volume constraint because the number of bees is constant during the optimization process in the standard ABCA<sup>[14,22-24]</sup>. Then, a simple averaging scheme based on a limit value<sup>[22-24]</sup> is applied to avoid local minima using Eq. (22).

$$\begin{aligned}
 \text{fit}_e^k &= \begin{cases} \frac{\text{fit}_e^k + \text{fit}_e^{k-1}}{2} & (\text{if } k \neq \text{limit value step}) \\ \text{fit}_e^k & (\text{if } k = \text{limit value step}) \end{cases} \\
 \text{limit value step} &= \text{limit value} \times \text{step} (= 1, 2, 3, \dots) \quad (22)
 \end{aligned}$$

where *limit value* is a predetermined value. The *limit value* is set to between 10 and 15 for topology optimization<sup>[22-24]</sup>. The value is set to between 5 and 10 for topological shape optimization. This is because solid elements can move in the defined boundary elements, which makes the convergence rate of the method slower. Therefore, the scheme should be performed for topological shape optimization more often than that of topology optimization<sup>[22-24]</sup>.

Step 7: Obtain an updated candidate solution through Steps 4 to 6. The waggle index update rule is then applied using Eq. (2). When  $k$  becomes between 15 and 20,  $\delta$  in Eq. (2) should become 0 since the waggle index  $I_i$  (that is, the trace of previous locations of elements occupied by employed bees) encourages the employed bee elements to try to move to the no boundary region. Therefore, employed bee  $ei$  (that is, the present location of elements occupied by employed bees) is

only used to calculate the sensitivity numbers from the prescribed iteration number.

Step 8: Calculate the objective function based on the obtained candidate solution, and calculate the sensitivity number based on the  $I_i$ . After calculating the sensitivity number, the mesh-independency filter scheme<sup>[8,22-24]</sup> using Eq. (23) is employed to prevent a checkerboard pattern,

$$\begin{aligned}
 \alpha_e &= \frac{\sum_{n=1}^M w(r_{en}) \alpha_n}{\sum_{n=1}^M w(r_{en})}, \\
 w(r_{en}) &= r_{\min} - r_{en} \quad (n = 1, 2, \dots, M) \quad (23)
 \end{aligned}$$

where  $M$  is the total number of nodes in the sub-domain,  $w(r_{en})$  is the linear weight factor,  $r_{en}$  is the distance between the center of the  $e$ -th element and the  $n$ -th node,  $\alpha_n$  is the sensitivity number of  $n$ -th node, and  $r_{\min}$  is the length scale parameter.

Step 9: Check whether the updated candidate solution has converged or not using Eq. (24).

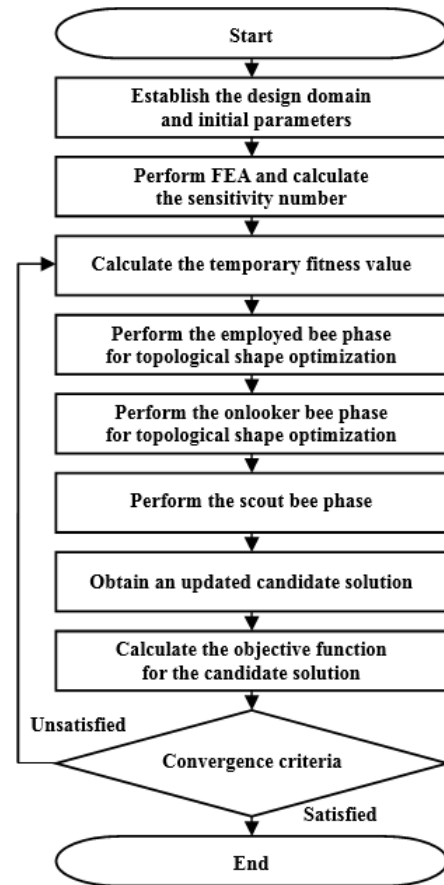


Fig. 2 Flow chart of the suggested ABCA

$$error = \frac{\left| \sum_{i=1}^{N'} (W_{k-i+1}^C - W_{k-N'-i+1}^C) \right|}{\sum_{i=1}^{N'} W_{k-i+1}^C} \leq \tau \quad (24)$$

where  $\tau$  is the allowable convergence tolerance,  $W^C$  is the complementary work,  $N'$  is the integer number resulting in a converged objective function. In this paper,  $\tau$  is set to 0.001, and  $N'$  is set to 5 in order to make the change in the objective function sufficiently small over the last 10 iterations.

If the solution is not converged, go to Step 3 and repeat the above steps until the solution is converged<sup>[8,22-24]</sup>. The flow chart of the proposed method is shown in Fig. 2.

### 4. Numerical Examples

In order to examine the performance of the ABCA for topological shape optimization, which is the proposed method, numerical examples are provided to compare with the discrete LSM<sup>[25]</sup> and the ABCA for topology optimization<sup>[23]</sup>. In this paper, three kinds of nonlinear cases, such as the geometrically nonlinear case, the materially nonlinear case, and both geometrically and materially nonlinear cases are considered. Since the ABCA is the stochastic method, each example using the ABCAs is performed for 5 runs. Objective functions of the ABCAs are mean values of 5 runs and standard deviations are provided.

#### 4.1 Simply Supported Beam

A simply supported beam measuring 0.8 m × 0.2 m × 0.001 m and subjected to 200 N at the center of the top surface is shown in Fig. 3. The design domain is divided into 160 × 40 by rectangular finite elements. The material properties are assumed to have Young's modulus of 1 GPa, Poisson's ratio of 0.3 and yield strength of 2 MPa. The materially nonlinear model is assumed to be a bilinear material and the tangent elastic modulus is 0.2 GPa. The limit value is set to 5, the  $\delta$  is set to 0.8, and the rmin is set to between 1.5 and 3.0. The objective of this problem is to determine the topological shape design having the minimum value of complementary work while satisfying a volume constraint of 20%.

The optimized designs of the discrete LSM<sup>[25]</sup>, the ABCA for topology optimization<sup>[23]</sup> and the ABCA for topological shape optimization are shown in Table 2. These results show that optimal designs based on the discrete LSM, the ABCA for

topology optimization and the ABCA for topological shape optimization are almost equal, and the convergence rate of the ABCA for topological shape optimization is the fastest among

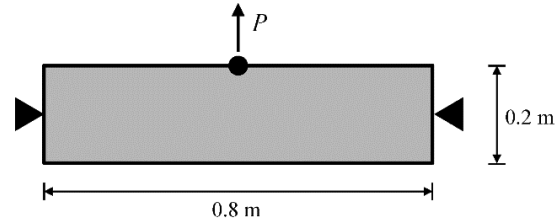


Fig. 3 Problem definition of the simply supported beam

Table 2 Comparison of optimized designs using the discrete LSM and the ABCAs for the simply supported beam

Linear / Nonlinear case	Discrete LSM <sup>[25]</sup>	ABCA for topology optimization <sup>[23]</sup>	ABCA for topological shape optimization
Linear	 Iter.: 130 Obj.: 1.7099 J	 Iter.: 49 Obj.: 1.7283 J Stdev.: 0.0119	 Iter.: 40 Obj.: 1.7107 J Stdev.: 0.0103
Geometrically nonlinear	 Iter.: 143 Obj.: 1.5746 J	 Iter.: 48 Obj.: 1.5963 J Stdev.: 0.0110	 Iter.: 48 Obj.: 1.5873 J Stdev.: 0.0108
Materially nonlinear	 Iter.: 112 Obj.: 8.3470 J	 Iter.: 43 Obj.: 8.4077 J Stdev.: 0.0138	 Iter.: 35 Obj.: 8.3512 J Stdev.: 0.0119
Both geometrically and materially nonlinear	 Iter.: 149 Obj.: 5.5300 J	 Iter.: 46 Obj.: 5.6112 J Stdev.: 0.0122	 Iter.: 43 Obj.: 5.5793 J Stdev.: 0.0106

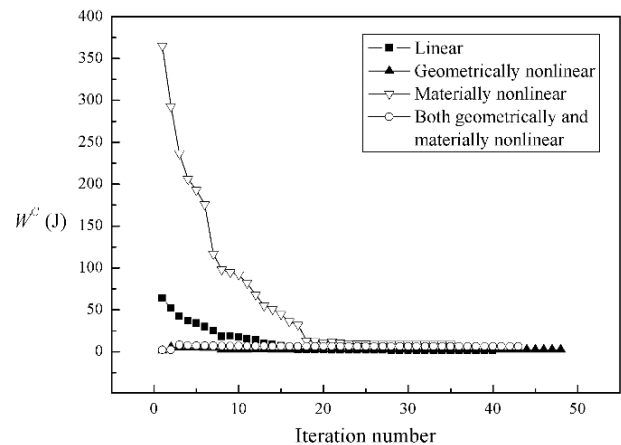


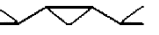

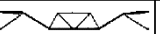
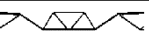


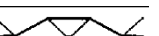





Fig. 4 Iteration history of the complementary work for the simply supported beam

**Table 3 Comparison of optimized designs using the discrete LSM and the ABCAs for the clamped beam**

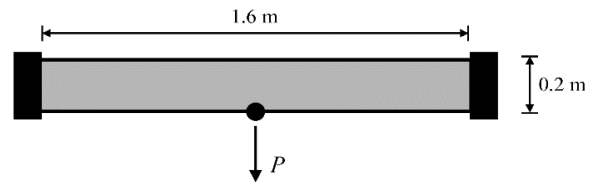
Linear / Nonlinear case	Discrete LSM <sup>[25]</sup>	ABCA for topology optimization <sup>[23]</sup>	ABCA for topological shape optimization
Linear	 Iter.: 170 Obj.: 0.2449 J	 Iter.: 53 Obj.: 0.2506 J Stdev.: 0.0113	 Iter.: 41 Obj.: 0.2481 J Stdev.: 0.0097
Geometrically nonlinear	 Iter.: 166 Obj.: 0.2341 J	 Iter.: 53 Obj.: 0.2401 J Stdev.: 0.0108	 Iter.: 52 Obj.: 0.2358 J Stdev.: 0.0098
Materially nonlinear	 Iter.: 177 Obj.: 0.8499 J	 Iter.: 59 Obj.: 0.8770 J Stdev.: 0.0119	 Iter.: 47 Obj.: 0.8561 J Stdev.: 0.0103
Both geometrically and materially nonlinear	 Iter.: 117 Obj.: 0.8113 J	 Iter.: 52 Obj.: 0.8300 J Stdev.: 0.0118	 Iter.: 44 Obj.: 0.8241 J Stdev.: 0.0101

the methods. Fig. 4 shows the iteration history of the complementary work for the simply supported beam. From the figure, it can be verified that the values are converged stably.

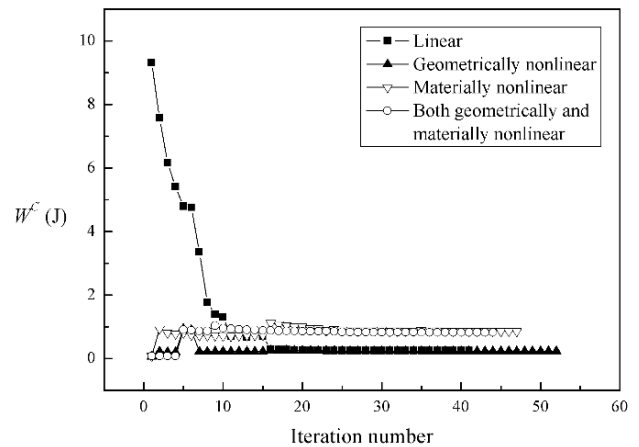
The optimized designs of the discrete LSM<sup>[25]</sup>, the ABCA for topology optimization<sup>[23]</sup> and the ABCA for topological shape optimization are shown in Table 3. These results show that optimal designs based on the discrete LSM, the ABCA for topology optimization and the ABCA for topological shape optimization are almost equal, and the convergence rate of the ABCA for topological shape optimization is the fastest among the methods.

#### 4.2 Clamped Beam

A clamped beam measuring 1.6 m × 0.2 m × 0.01 m and subjected to 30 N at the center of the bottom surface is shown in Fig. 5. The design domain is divided into 240 × 30 by rectangular finite elements. The material properties are assumed to have Young's modulus of 30 MPa, Poisson's ratio of 0.3 and yield strength of 0.06 MPa. The materially nonlinear model is assumed to be a power-law material model having a work-hardening exponent of 0.5. That is, the stress-strain relationship after yielding is  $\sigma = 1.34\epsilon^{0.5}$ . The *limit value* is set to 5, the  $\delta$  is set to 0.8, and the  $r_{\min}$  is set to between 1.5 and 3.0. The objective of this problem is to



**Fig. 5 Problem definition of the clamped beam**



**Fig. 6 Iteration history of the complementary work for the clamped beam**

determine the topological shape design having minimum value of complementary work while satisfying a volume constraint of 20%. Fig. 6 shows the iteration history of the complementary work for the clamped beam. From the figure, it can be verified that the values are converged stably.

#### 4.3 Discussions

The *BEI* is first employed for the topological shape optimization of linear and nonlinear problems, but it can be found that the *BEI* is not sufficient to properly solve the solution of nonlinear problems. This is because the defined boundary elements using the *BEI* are too narrow. In order to address this problem, the *IBEI* is suggested. Although the *BEI* defines the solid and void elements, which are on each layer at the both sides of the boundary line as the boundary elements, the *IBEI* defines the elements which are on double layers as the boundary elements. Therefore, the defined boundary elements can be expanded considerably, and nonlinear problems can also be solved appropriately based on the *IBEI*.

In view of the accuracy of convergence, the discrete LSM and the ABCA for topological shape optimization yield a better solution than the ABCA for topology optimization. The reason is that the discrete LSM and the ABCA for topological shape optimization have the effect of shape optimization.



The effect could be easily confirmed from Table 4. From the optimized design by ABCA for topology optimization, it can be verified that the method makes the unnecessary small sized holes in the structure and solid bumps on the surface. However, the suggested ABCA in this paper could create optimum number of the holes and alleviate the surface roughness as shown because the method searches the solutions in only boundary area (shape optimization) based on *IBEI* unlike searching solutions in overall design domain by ABCA for topology optimization.

Also, the discrete LSM can find a somewhat better solution for topological shape optimization than the ABCA for topological shape optimization. Although the ABCA for topological shape optimization uses only the shape sensitivity information, the discrete LSM uses a normal vector of structural boundary as well as shape sensitivity information. It can thus be found that the normal vector of the structural boundary provides information about better solutions. However, the differences between objective functions using the discrete LSM and the ABCA for topological shape optimization are insignificant.

It can be verified that the convergence rate of the ABCA for topological shape optimization is faster than the discrete LSM and the ABCA for topology optimization (except in the geometrically nonlinear case). This is because the searching domain of the suggested ABCA is defined continuously, so the searching domain is much narrower than that of the ABCA for topology optimization. Also, since the discrete LSM performs the optimization based on the Hamilton-Jacobi equation, which can evolve the geometry only from the existing boundary based on the shape and topological sensitivities, the convergence rate of the suggested ABCA that

searches the solutions based on continuously updated boundary elements (region) is faster than the discrete LSM.

In the geometrically nonlinear case, the convergence rate of the ABCA for topological shape optimization is not significantly improved compared with that of the ABCA for topology optimization. From this, it follows that the searching domain of the suggested ABCA is still narrow, although the searching domain is expanded by the *IBEI*. Despite of the lack in improvement of the convergence rate of the geometrically nonlinear case, it can be verified that the shape optimization is well carried out by the ABCA for topological shape optimization from the improved objective function compared with that of the ABCA for topology optimization. Even though it is possible that it might be slow to find an optimal topology for a relatively complicated structure such as the optimized solution for the geometrically nonlinear case, the suggested ABCA reflects the substantial effect of shape optimization.




The discrete LSM requires initial holes or weighting factors for topological sensitivity<sup>[3,6,25]</sup> in order to create new holes in the structures. However, the number of initial holes or the value of the weighting factor significantly affects the optimized solutions. Therefore, the number of initial holes or the value of the weighting factor is appropriately predetermined for the discrete LSM. On the other hand, the suggested ABCA can create holes naturally without any initial holes or topological sensitivity because the solid elements are distributed to efficient regions in the overall design domain, although only the boundary elements are optimized. Therefore, the suggested method is more efficient than the discrete LSM.

### 5. Conclusions

In this study, a method for topological shape optimization for nonlinear structures based on the ABCA is suggested. From the results of the numerical examples, the following conclusions are made:

- (1) To perform the topological shape optimization for linear and nonlinear structures, a variable called the “Improved Boundary Element Indicator (*IBEI*)” is employed.
- (2) The suggested method can naturally create holes in the structure without any initial holes or topological sensitivity, although only the boundary elements are optimized.
- (3) The objective function of the suggested ABCA is better

**Table 4 Comparison of optimized simply supported beams in the materially nonlinear case**

Method	Optimized design
Discrete LSM <sup>[25]</sup>	
ABCA for topology optimization <sup>[23]</sup>	
ABCA for topological shape optimization	

than that of the ABCA for topology optimization, and similar to that of the discrete LSM.

(4) It can be found that the convergence rate of the suggested ABCA is improved up to more than 60% of the discrete LSM and 5% of the ABCA for topology optimization (except for the geometrically nonlinear case).

## References

- [1] Sethian, J. A., Wiegmann, A., 2000, Structural Boundary Design via Level Set and Immersed Interface Methods, *J. Comput. Phys.*, 163:2 489-528.
- [2] Bourdin, B., Chambolle, A., 2003, Design-dependent Loads in Topology Optimization, *ESAIM: Control, Optim. Calc. Var.*, 9 19-48.
- [3] Allaire, G., Jouve, F., Toader, A.-M., 2004, Structural Optimization Using Sensitivity Analysis and a Level-set Method, *J. Comput. Phys.*, 194:1 363-393.
- [4] Allaire, G., Jouve, F., 2008, Minimum Stress Optimal Design with the Level Set Method, *Eng. Anal. Bound. Elem.*, 32:11 909-918.
- [5] Zhou, S., Wang, M. Y., 2007, Multimaterial Structural Topology Optimization with a Generalized Cahn-Hilliard Model of Multiphase Transition, *Struct. Multidiscip. Optim.*, 33:2 89-111.
- [6] Takezawa, A., Nishiwaki, S., Kitamura, M., 2010, Shape and Topology Optimization Based on the Phase Field Method and Sensitivity Analysis, *J. Comput. Phys.*, 229:7 2697-2718.
- [7] Behrou, R., Lawry, M., Maute, K., 2017, Level Set Topology Optimization of Structural Problems with Interface Cohesion, *Int. J. Nemer. Method Eng.*, 112:8 990-1016.
- [8] Huang, X., Xie, Y. M., 2010, *Evolutionary Topology Optimization of Continuum Structures: Methods and Applications*, John Wiley & Sons, Chichester, United Kingdom.
- [9] Kwak, J., Cho, S., 2005, Topological Shape Optimization of Geometrically Nonlinear Structures Using Level Set Method, *Comput. Struct.*, 83:27 2257-2268.
- [10] Cho, S., Ha, S. H., Kim, M. G., 2006, Level Set Based Shape Optimization of Geometrically Nonlinear Structures, *IUTAM Symposium on Topological Design Optimization of Structures, Machines and Materials*, 217-226.
- [11] Ha, S.-H., Cho, S., 2008, Level Set Based Topological Shape Optimization of Geometrically Nonlinear Structures Using Unstructured Mesh, *Comput. Struct.*, 86:13-14 1447-1455.
- [12] Penzler, P., Rumpf, M., Wirth, B., 2012, A Phase-field Model for Compliance Shape Optimization in Nonlinear Elasticity, *ESAIM: Control, Optim. Calc. Var.*, 18:1 229-258.
- [13] Myśliński, A., Koniarski, K., 2014, Phase Field Regularized Level Set Approach in Topology Optimization of Variational Inequalities, *Methods and Models in Automation and Robotics (MMAR), 2014 19th International Conference on*, 514-519.
- [14] Karaboga, D., Basturk, B., 2008, On the Performance of Artificial Bee Colony (ABC) Algorithm, *Appl. Soft Comput.*, 8:1 687-697.
- [15] Storn, R., Price, K., 1997, Differential Evolution – A Simple and Efficient Heuristic for Global Optimization over Continuous Spaces, *J. Glob. Optim.*, 11:4 341-359.
- [16] Kennedy, J., Eberhart, R., 1995, Particle Swarm Optimization, *Neural Networks, Proceedings, IEEE International Conference on*, 1942-1948.
- [17] Bäck, T., 1996, *Evolutionary Algorithms in Theory and Practice: Evolution Strategies, Evolutionary Programming, Genetic Algorithms*, Oxford University Press.
- [18] Çavdar, T., Mohammad, M., Milani, R. A., 2013, A New Heuristic Approach for Inverse Kinematics of Robot Arms, *Adv. Sci. Lett.*, 19:1 329-333.
- [19] Apalak, M. K., Karaboga, D., Akay, B., 2014, The Artificial Bee Colony Algorithm in Layer Optimization for the Maximum Fundamental Frequency of Symmetrical Laminated Composite Plates, *Eng. Optim.*, 46:3 420-437.
- [20] Kim, Y.-H., Han, S.-Y., 2014, A Shape Optimization Scheme for Static Stiffness Problems, *Proceedings of the International Conference of Manufacturing Technology Engineers (ICMTE) 2014*, 183.
- [21] Kim, Y.-H., Han, S.-Y., 2015, A Shape Optimization Procedure Based on the Artificial Bee Colony Algorithm, *Int. J. Precis. Eng. Manuf.*, 16:8 1825-1831.
- [22] Park, J.-Y., Han, S.-Y., 2013, Swarm Intelligence Topology Optimization Based on Artificial Bee Colony Algorithm, *Int. J. Precis. Eng. Manuf.*, 14:1 115-121.
- [23] Park, J.-Y., Han, S.-Y., 2015, Topology Optimization for Nonlinear Structural Problems Based on Artificial Bee Colony Algorithm, *Int. J. Precis. Eng. Manuf.*, 16:1 91-97.
- [24] Park, J.-Y., Han, S.-Y., 2013, Application of Artificial Bee Colony Algorithm to Topology Optimization for Dynamic Stiffness Problems, *Comput. Math. Appl.*, 66:10 1879-1891.
- [25] Challis, V. J., 2010, A Discrete Level-set Topology Optimization Code Written in Matlab, *Struct. Multidiscip. Optim.*, 41:3 453-464.
- [26] Kaveh, A., Hassani, B., Shojaei, S., Tavakkoli, S. M., 2008, Structural Topology Optimization Using Ant Colony Methodology, *Eng. Struct.*, 30:9 2559-2565.